

Cell Reports, Volume 43

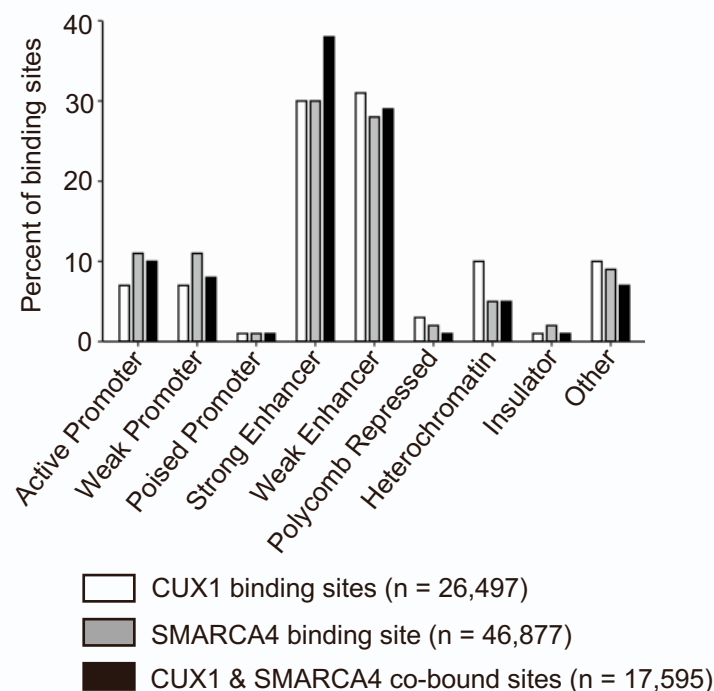
Supplemental information

**CUX1 regulates human hematopoietic stem cell
chromatin accessibility via the BAF complex**

Weihan Liu, Jeffrey L. Kurkewich, Angela Stoddart, Saira Khan, Dhivyaa Anandan, Alexandre N. Gaubil, Donald J. Wolfeher, Lia Jueng, Stephen J. Kron, and Megan E. McNerney

Supplemental Figure 1

A. Distribution of K562 CUX1 & SMARCA4 binding sites



B. Percent of binding sites co-occupied by lineage-specific hematopoietic TFs in K562

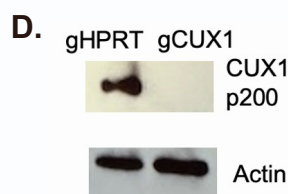
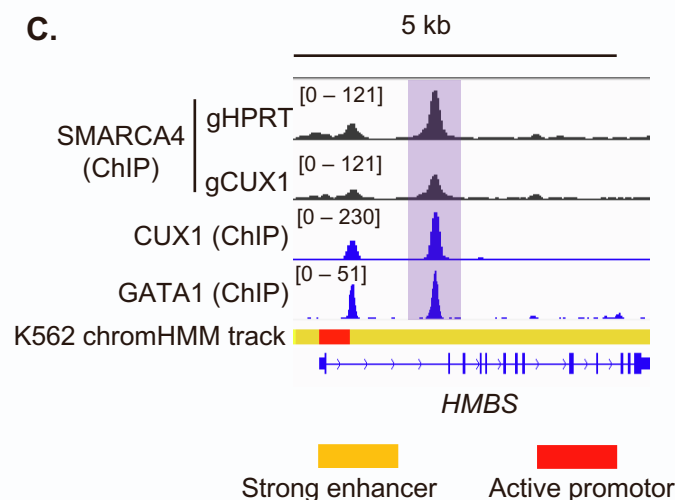
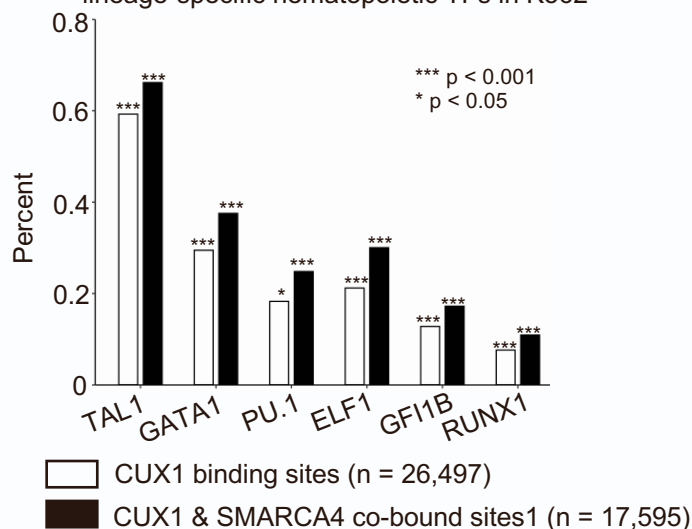


Figure S1. Related to Figure 1. Features of CUX1 and SMARCA4 binding targets in K562 cells

(A) Chromatin state annotation of all CUX1 binding sites (n=26,497), all SMARCA4 binding sites (n=46,877) and CUX1 and SMARCA4 overlapping sites (n=17,595) via intersecting binding sites with the K562 ChromHMM track^{1,2}. **(B)** Percent of CUX1 binding sites and CUX1/SMARCA4 co-bound sites from ChIP-seq co-occupied by lineage specific hematopoietic TFs (all pairwise comparisons of overlap are significant by hypergeometric test, $p < 0.05$). All hematopoietic TF ChIP-seq binding sites are obtained from ENCODE database^{3,4}. **(C)** IGV analysis of ChIP-seq tracks at the *HMBS* erythroid gene⁵. Tracks shown are normalized ChIP-seq signal across 2 replicates (RPKM) for K562 SMARCA4 gHPRT, gCUX1, CUX1 and GATA1, along with K562 chromHMM chromatin state annotations. **(D)** Western blot (n = 3 biological replicates) showing CUX1 protein deletion for the second independent K562 gCUX1 clone targeting *CUX1* exon 6.

Supplemental Figure 2

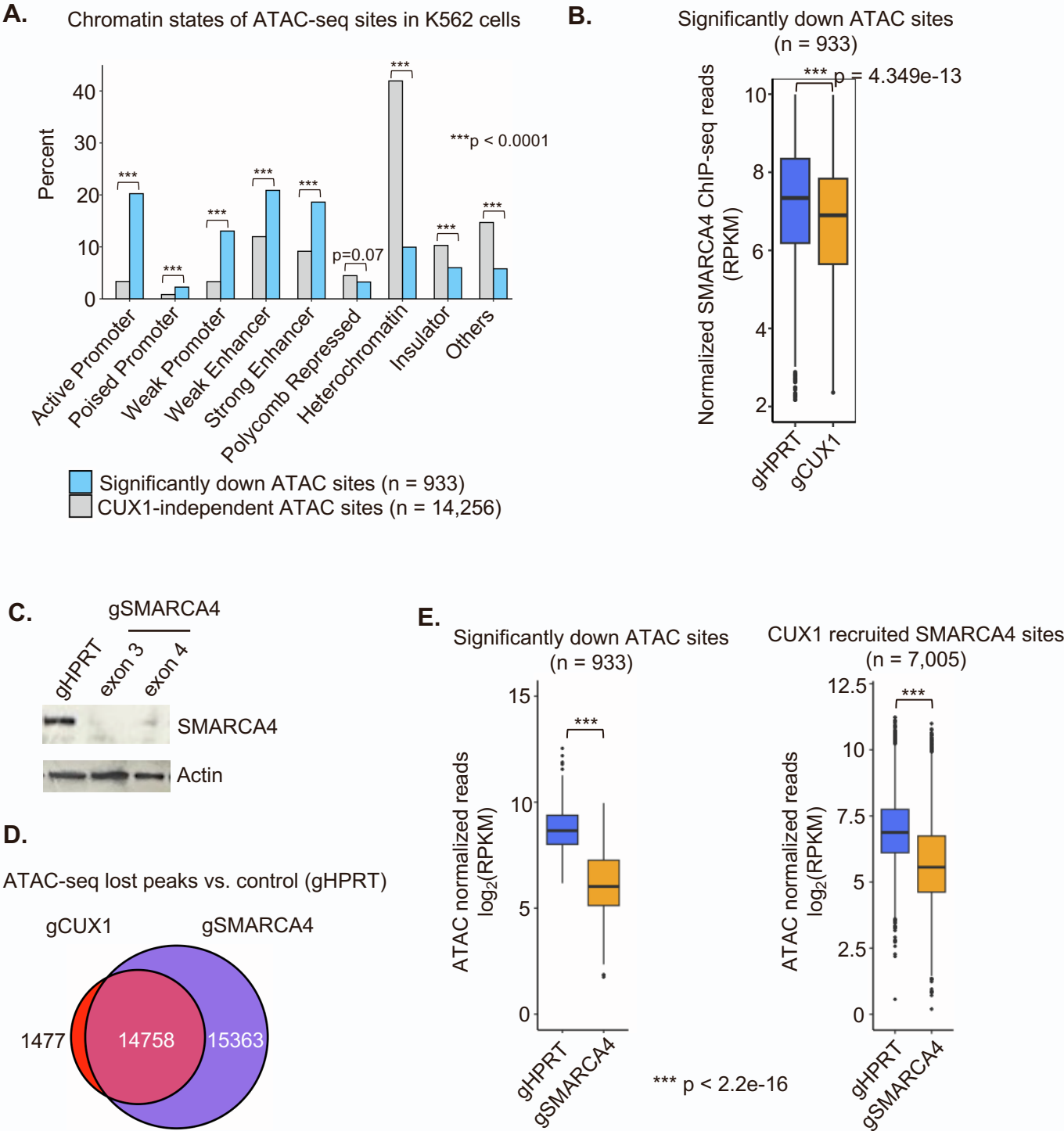


Figure S2. Related to Figure 2. Features of ATAC-seq sites in K562 cells.

(A) Distribution of K562 chromHMM chromatin state^{1,2} of the sites where accessibility are significantly downregulated after CUX1 loss (n=933, blue, FDR<0.05, $\log_2\text{FC}<-1$) and the ATAC sites where accessibility are not dependent on CUX1 (n=14,256, grey, FDR>0.1, $|\log_2\text{FC}|<0.5$). **(B)** Normalized SMARCA4 ChIP-seq reads (gCUX1 vs control gHPRT) at the significantly down ATAC sites (n = 933) from Figure 2A. **(C)** Western blot (n = 2 biological replicates) showing SMARCA4 protein deletion using two independent clones with gRNAs targeting exon 3 and 4 of *SMARCA4* gene. **(D)** Overlap of the lost ATAC-seq peaks in gSMARCA4 vs. gCUX1 samples compared to the control gHPRT (n = 2 biological replicates, IDR < 0.05). “Lost peaks” refer to the peaks present in gHPRT but are absent in the knockout conditions. **(E)** ATAC-seq signal (n = 3 biological replicates, control gHPRT vs. gSMARCA4) at the significantly down ATAC sites (n = 933) from Figure 2A and CUX1 recruited SMARCA4 sites (n = 7,005) from Figure 2E. Statistical significance for **(B)** and **(E)** was calculated using Wilcoxon rank-sum test.

Supplemental Figure 3

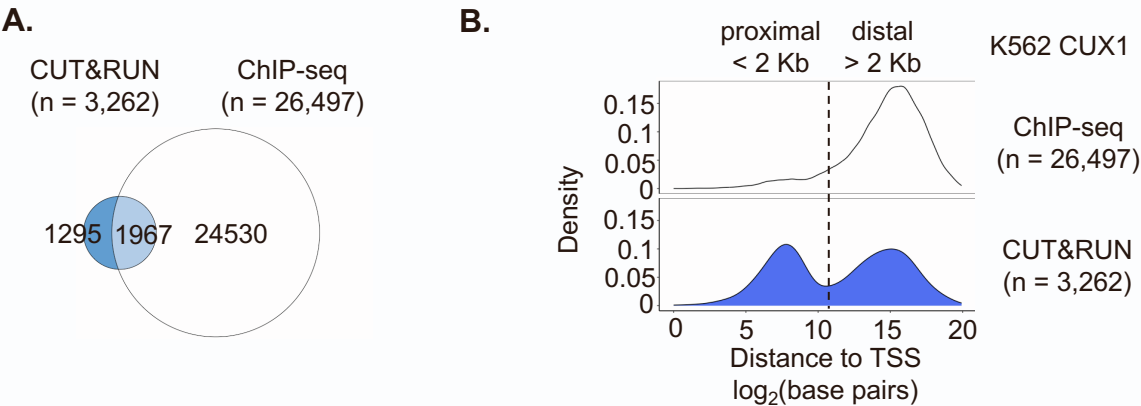
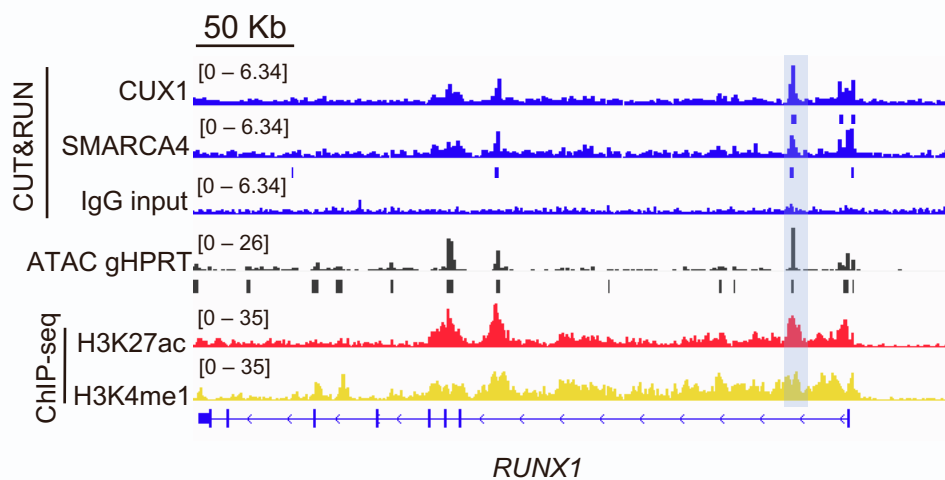
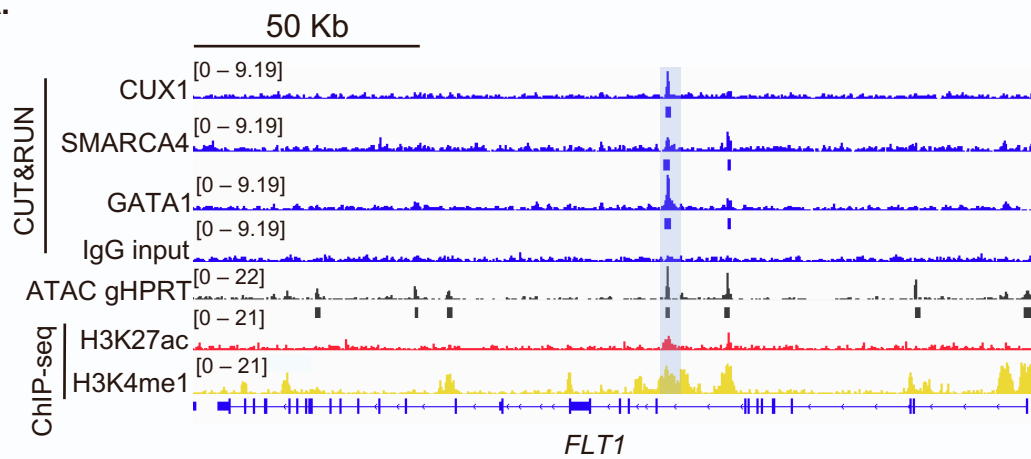


Figure S3. Related to Figure 3. Discrepancy between CUT&RUN and ChIP-seq peak calling in K562

(A) Overlap of CUT&RUN and ChIP-seq called CUX1 peaks in K562 (IDR < 0.05, n = 2 biological replicates). **(B)** Distance to the nearest TSS for CUX1 binding sites in K562 identified by ChIP-seq and CUT&RUN

Supplemental Figure 4

A.



B.

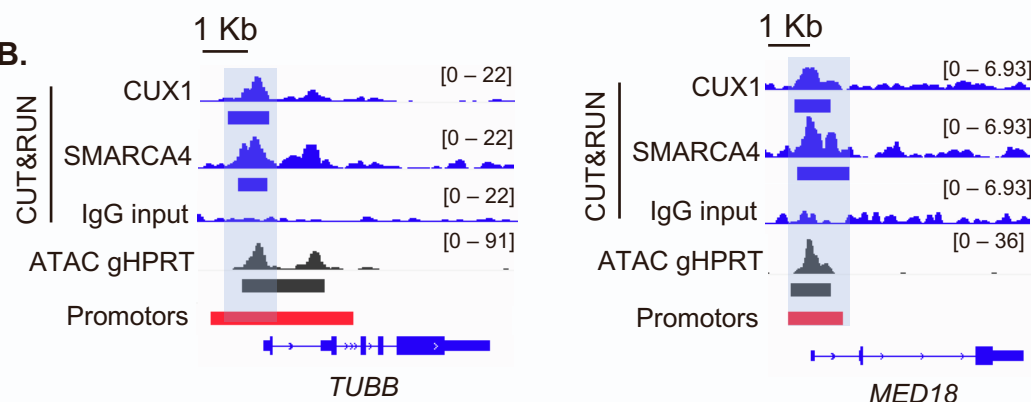
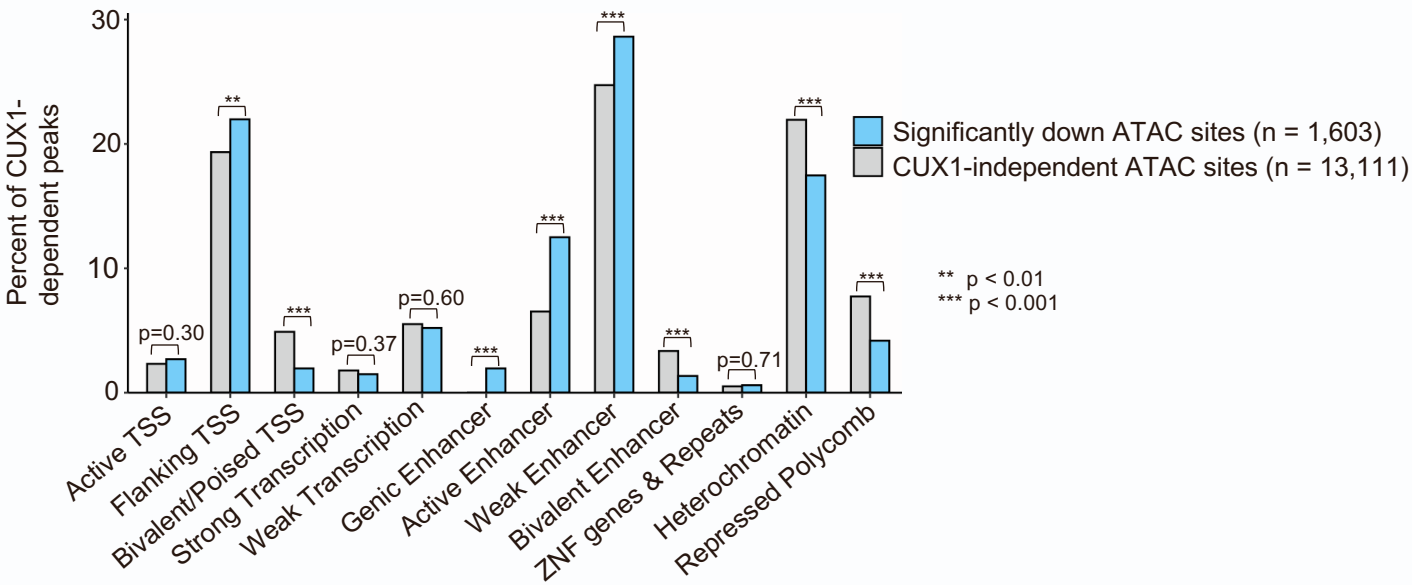


Figure S4. Related to Figure 3. Example genome snapshots of CUX1 and SMARCA4 co-occupancy in primary human CD34⁺ HSPC.

IGV genome snapshots of human CD34⁺ HSPC CUT&RUN data showing CUX1 and SMARCA4 co-occupancy at **(A)** enhancers of hematopoietic lineage-specifying genes *FLT1* and *RUNX1*⁶⁻⁸. ATAC-seq gHPRT control track and active enhancer-specific histone modifications H3K27ac and H3K4me1 tracks obtained from Roadmap Epigenomics are added. **(B)** CUX1 and SMARCA4 co-occupancy at promoters of essential genes involved in mitosis *TUBB*, and *MED18*, which is a subunit of the mediator complex that is essential in DNA transcription^{9,10}. Promoter annotation labeled by Roadmap Epigenomics are added. Highlighted areas are CUX1, SMARCA4 and ATAC-seq peaks called by MACS2 (solid rectangles, IDR < 0.05)

Supplemental Figure 5

A. Chromatin states of ATAC-seq sites in primary human CD34+ HSPC



B.

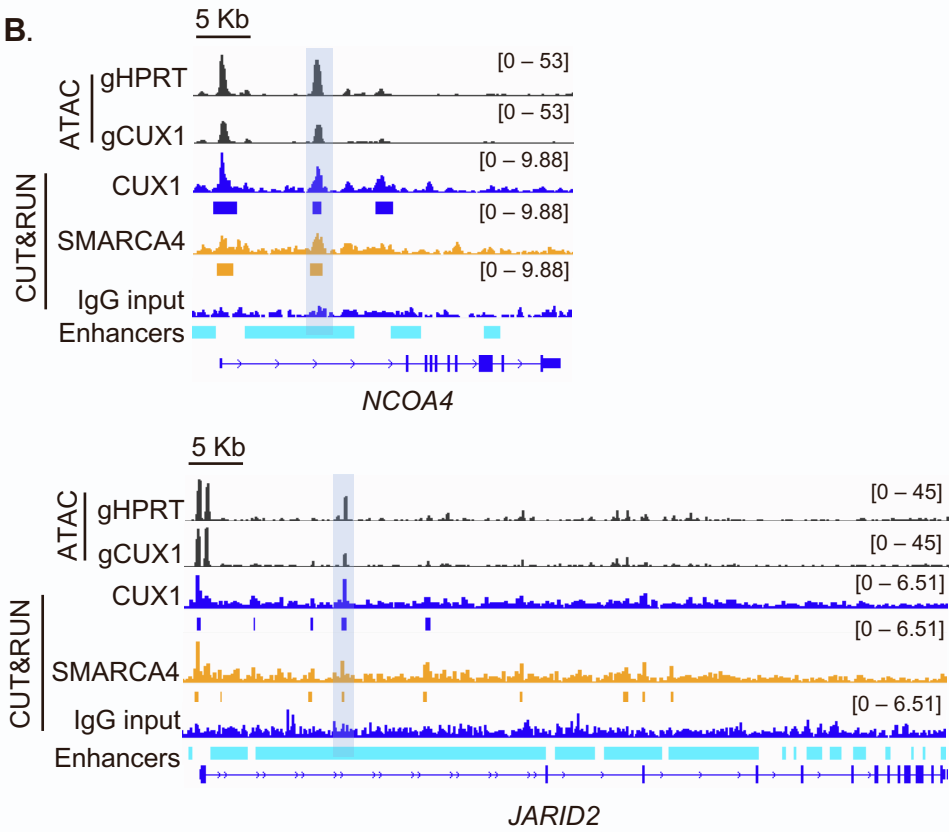


Figure S5. Related to Figure 4. Chromatin state and example genome snapshots of ATAC-seq sites in primary human CD34+ HSPC.

(A) Distribution of chromHMM chromatin state¹¹ of the peaks whose accessibility are significantly downregulated after CUX1 loss (n=1,603, blue, FDR<0.05, log₂FC<-1) and the ATAC sites whose accessibility are not dependent on CUX1 (n=13,111, grey, FDR>0.1, |log₂FC|<0.5). (B) IGV analysis of normalized ATAC-seq signal (RPKM) tracks of gHPRT and gCUX1 cells at hematopoiesis-regulating genes *NCOA4*¹² and *JARID2*^{13,14}. Normalized CUX1 and SMARCA4 binding signal (RPKM) from CUT&RUN experiment are shown along with CD34+ HSPC chromHMM enhancer annotations. (*NCOA4* lost site log₂FC=-1.16, FDR=0.073; *JARID2* lost site log₂FC=-1.10, FDR=0.070)

Supplemental Figure 6

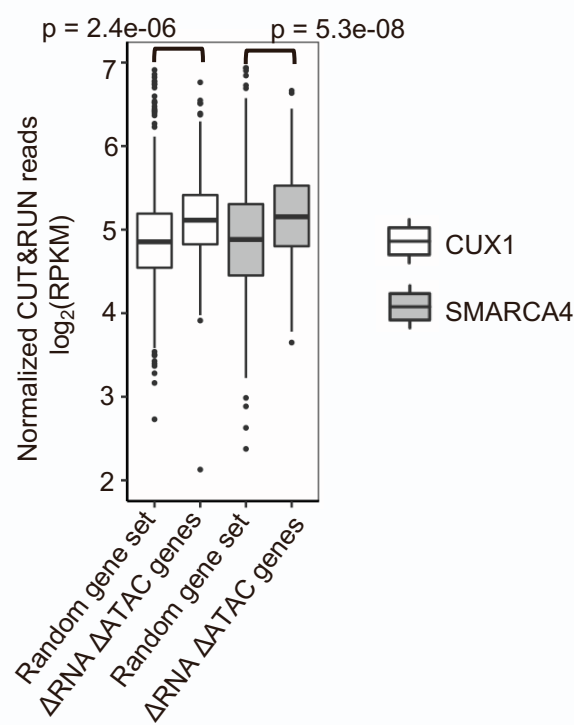


Figure S6. Related to Figure 4. CUX1 and SMARCA4 binding intensity at genes with concordant chromatin accessibility and RNA expression change in primary human CD34+ HSPC.

A quantitative comparison of CD34+ HSPC normalized CUT&RUN reads of CUX1 (left) and SMARCA4 (right) at the sites with simultaneously significant changes in RNA expression and chromatin accessibility from **Figure 4C** (n=406), vs. the control, which are size-matched regions associated with randomly sampled genes (n=406) from csaw results.

SUPPLEMENTAL REFERENCES

1. Ernst, J., and Kellis, M. (2010). Discovery and characterization of chromatin states for systematic annotation of the human genome. *Nat. Biotechnol.* 28, 817–825. 10.1038/nbt.1662.
2. Ernst, J., Kheradpour, P., Mikkelsen, T.S., Shores, N., Ward, L.D., Epstein, C.B., Zhang, X., Wang, L., Issner, R., Coyne, M., et al. (2011). Mapping and analysis of chromatin state dynamics in nine human cell types. *Nature* 473, 43–49. 10.1038/nature09906.
3. ENCODE Project Consortium (2012). An integrated encyclopedia of DNA elements in the human genome. *Nature* 489, 57–74. 10.1038/nature11247.
4. Luo, Y., Hitz, B.C., Gabdank, I., Hilton, J.A., Kagda, M.S., Lam, B., Myers, Z., Sud, P., Jou, J., Lin, K., et al. (2020). New developments on the Encyclopedia of DNA Elements (ENCODE) data portal. *Nucleic Acids Res.* 48, D882–D889. 10.1093/nar/gkz1062.
5. Elder, G.H. (1998). Genetic Defects in the Porphyrrias: Types and Significance. *Clin. Dermatol.* 16, 225–233. 10.1016/S0738-081X(97)00202-2.
6. Nottingham, W.T., Jarratt, A., Burgess, M., Speck, C.L., Cheng, J.-F., Prabhakar, S., Rubin, E.M., Li, P.-S., Sloane-Stanley, J., Kong-a-San, J., et al. (2007). Runx1-mediated hematopoietic stem-cell emergence is controlled by a Gata/Ets/SCL-regulated enhancer. *Blood* 110, 4188–4197. 10.1182/blood-2007-07-100883.
7. Bee, T., Ashley, E.L.K., Bickley, S.R.B., Jarratt, A., Li, P.-S., Sloane-Stanley, J., Göttgens, B., and de Bruijn, M.F.T.R. (2009). The mouse Runx1 +23 hematopoietic stem cell enhancer confers hematopoietic specificity to both Runx1 promoters. *Blood* 113, 5121–5124. 10.1182/blood-2008-12-193003.
8. Lee, D., Shi, M., Moran, J., Wall, M., Zhang, J., Liu, J., Fitzgerald, D., Kyono, Y., Ma, L., White, K.P., et al. (2020). STARRPeaker: uniform processing and accurate identification of STARR-seq active regions. *Genome Biol.* 21, 298. 10.1186/s13059-020-02194-x.
9. Sato, S., Tomomori-Sato, C., Banks, C.A.S., Sorokina, I., Parmely, T.J., Kong, S.E., Jin, J., Cai, Y., Lane, W.S., Brower, C.S., et al. (2003). Identification of mammalian Mediator subunits with similarities to yeast Mediator subunits Srb5, Srb6, Med11, and Rox3. *J. Biol. Chem.* 278, 15123–15127. 10.1074/jbc.C300054200.
10. Ferreira, L.T., Figueiredo, A.C., Orr, B., Lopes, D., and Maiato, H. (2018). Dissecting the role of the tubulin code in mitosis. *Methods Cell Biol.* 144, 33–74. 10.1016/bs.mcb.2018.03.040.
11. Kundaje, A., Meuleman, W., Ernst, J., Bilenky, M., Yen, A., Heravi-Moussavi, A., Kheradpour, P., Zhang, Z., Wang, J., Ziller, M.J., et al. (2015). Integrative analysis of 111 reference human epigenomes. *Nature* 518, 317–330. 10.1038/nature14248.
12. Mancias, J.D., Pontano Vaites, L., Nissim, S., Biancur, D.E., Kim, A.J., Wang, X., Liu, Y., Goessling, W., Kimmelman, A.C., and Harper, J.W. (2015). Ferritinophagy via NCOA4 is required for erythropoiesis and is regulated by iron dependent HERC2-mediated proteolysis. *eLife* 4, e10308. 10.7554/eLife.10308.
13. Kinkel, S.A., Galeev, R., Flensburg, C., Keniry, A., Breslin, K., Gilan, O., Lee, S., Liu, J., Chen, K., Gearing, L.J., et al. (2015). Jarid2 regulates hematopoietic stem cell function by acting with polycomb repressive complex 2. *Blood* 125, 1890–1900. 10.1182/blood-2014-10-603969.
14. Celik, H., Koh, W.K., Kramer, A.C., Ostrander, E.L., Mallaney, C., Fisher, D.A.C., Xiang, J., Wilson, W.C., Martens, A., Kothari, A., et al. (2018). JARID2 Functions as a Tumor Suppressor in Myeloid Neoplasms by Repressing Self-Renewal in Hematopoietic Progenitor Cells. *Cancer Cell* 34, 741–756.e8. 10.1016/j.ccell.2018.10.008.